J Low Temp Phys (2016) 184:405–411
DOI 10.1007/s10909-015-1466-8

Pile-Up Discrimination Algorithms for the HOLMES Experiment

E. Ferri[1] · B. Alpert[2] · D. Bennett[2] · M. Faverzani[1] · J. Fowler[2] · A. Giachero[1] · J. Hays-Wehle[2] · M. Maino[1] · A. Nucciotti[1] · A. Puiu[1] · J. Ullom[2]

Received: 29 September 2015 / Accepted: 31 December 2015 / Published online: 13 January 2016

Abstract The HOLMES experiment is a new large-scale experiment for the electron neutrino mass determination by means of the electron capture decay of ^{163}Ho. In such an experiment, random coincidence events are one of the main sources of background which impair the ability to identify the effect of a non-vanishing neutrino mass. In order to resolve these spurious events, detectors characterized by a fast response are needed as well as pile-up recognition algorithms. For that reason, we have developed a code for testing the discrimination efficiency of various algorithms in recognizing pile up events in dependence of the time separation between two pulses. The tests are performed on simulated realistic TES signals and noise. Indeed, the pulse profile is obtained by solving the two coupled differential equations which describe the response of the TES according to the Irwin-Hilton model. To these pulses, a noise waveform which takes into account all the noise sources regularly present in a real TES is added. The amplitude of the generated pulses is distributed as the ^{163}Ho calorimetric spectrum. Furthermore, the rise time of these pulses has been chosen taking into account the constraints given by both the bandwidth of the microwave multiplexing read out with a flux ramp demodulation and the bandwidth of the ADC boards currently available for ROACH2. Among the different rejection techniques evaluated, the Wiener Filter technique, a digital filter to gain time resolution, has shown an excellent pile-up rejection efficiency. The obtained time resolution closely matches the baseline specifications of the HOLMES experiment. We report here a description of our simulation code and a comparison of the different rejection techniques.

✉ E. Ferri
elena.ferri@mib.infn.it

1 Università di Milano-Bicocca and INFN Sez. di Milano-Bicocca, Milan, Italy

2 National Institute of Standards and Technology (NIST), Boulder, Colorado, USA

Keywords Pile-up discrimination algorithms · TES detectors

1 Introduction

The absolute neutrino mass scale is still an outstanding challenge in both particle physics and cosmology. To date, a powerful tool to directly measure the neutrino mass is the calorimetric measurement of the energy released in a nuclear process involving neutrino, like electron capture (EC) decay. In the last years, the progress on low-temperature detector technologies has allowed to design large-scale experiments aiming at pushing down the sensitivity on neutrino mass below 1 eV [1–3]. Indeed, in order to achieve a sub-eV sensitivity on m_ν a large number of detectors working in parallel and characterized by high energy and time resolution are required. Within this framework the European Research Council has recently funded HOLMES [2], a new large-scale experiment for measuring the neutrino mass by means of the EC decay of ^{163}Ho. In such experiment, random coincidence events are one of the main sources of background which impair the ability to identify the effect of a non-vanishing neutrino mass [4]. Besides using detectors with fast response as transition edge sensors (TESs), efficient pile-up recognition algorithms are needed to solve these spurious events. We present the code developed for testing the discrimination efficiency of various algorithms in recognizing pile up events in dependence of the time separation between two pulses.

2 TES Response

Accordingly the Irwin-Hilton model [5], the response of a TES detector is well described by two coupled differential equations. Each differential equation governs the evolution of a state variable: the thermal differential equation determines the temperature T, while the electrical differential equation determines the current I. Therefore, we have obtained the pulse profile (see left panel of Fig. 1) by solving the two coupled differential equations using a fourth-order Runge-Kutta method (RK4) and considering the transition resistance as proposed by Shank et al [6]. In this way, the TES non-linearity behavior is automatically taken into account (see right panel of Fig. 1). The rise time of the pulses is set by the electrical bandwidth of the read out circuit which is chosen to match the thermal response by selecting an inductance L.

To these pulses, a noise waveform which reckons with all the noise sources regularly present in a real TES is added. In fact, in addition to the thermodynamic fluctuations of TES state variables two noise terms must be considered: the Johnson noise due to the presence of the shunt resistance and the noise of the SQUID amplifier. The modeling of the TES noise (i.e., Irwin-Hilton model) is reported in [5]. In the left panel of Fig. 2 the noise contributions for a TES with $L = 24$ nH, which corresponds to a rise time of around 5 μs, are plotted from 1 Hz to 1 MHz. At low frequencies the total noise power spectrum is dominated by the thermal fluctuations between the TES and the thermal bath through the conductance G. The double roll-off is from the separate roll-off of the Johnson noise and thermal fluctuation noise. At high frequencies, the noise power spectrum is dominated by the SQUID amplifier noise which is flat in frequency. Since

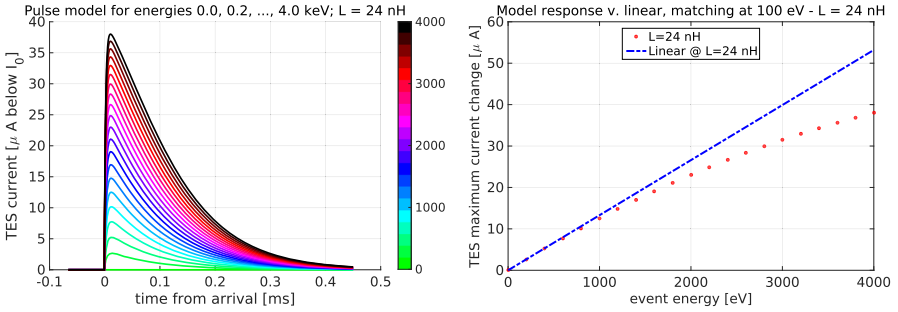

Fig. 1 *Left panel* pulse profiles corresponding to different energies from 0 to 4 keV for L =24 nH (different values of inductance L translate into different values of rise time as being set by the electrical bandwidth of the circuit). *Right panel* the non-linearity behavior of real TES pulses (Color figure online)

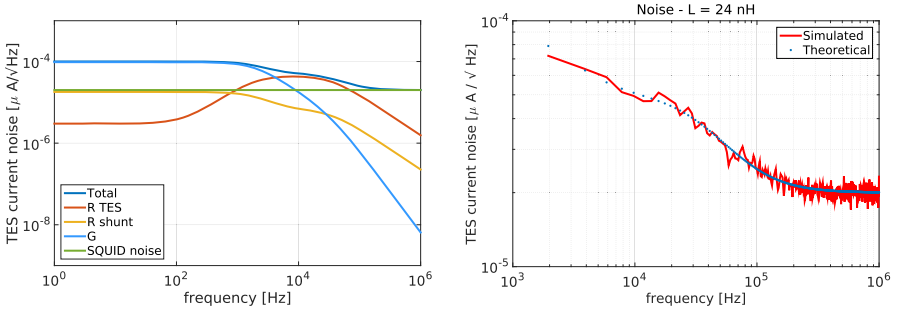

Fig. 2 *Left panel* the total noise power spectrum for a TES with L =24 nH and the contributions given by different components (thermodynamic fluctuations associated with R_{TES}—i.e., Johnson noise , thermodynamic fluctuations associated with the thermal impedance G—i.e., phonon noise , the Johnson noise due to the presence of the shunt resistance and the noise of the SQUID amplifier). *Right panel* comparison between the noise power spectrum calculated with 1 thousand of baselines and the total noise power spectrum modeling with the Irwin-Hilton model. The sampling frequency is 2 MHz and the record length is 1024, so that the minimum frequency is around 2 kHz (Color figure online)

it is quite flat up to the double roll-off, it could be well approximated by a white noise power spectrum processed with two first-order low-pass filters. For this reason, the noise baselines are simulated generating random sequences of Gaussian samples and processed with two low-pass software filters characterized by two different cut-off frequencies. In the right panel of Fig. 2, the superimposition of the noise power spectrum calculated with one thousand of simulated baselines and the total noise power spectrum simulated according to the Irwin-Hilton model is reported. In this case the minimum frequency of the noise power spectrum is around 2 kHz since the sampling rate is 2 MHz and the record length is 1024.

In our simulations, the pulses are generated with energies included in the energy range of the ^{163}Ho calorimetric spectrum and their frequencies are weighted on the shape of the spectrum. The de-excitation energy E_c distribution is

$$\frac{d\lambda_{EC}}{dE_c} = \frac{G_\beta^2}{4\pi^2}(Q - E_c)\sqrt{(Q - E_c)^2 - m_\nu^2} \times \sum_i n_i C_i \beta_i^2 B_i \frac{\Gamma_i}{2\pi} \frac{1}{(E_c - E_i)^2 + \Gamma_i^2/4} \quad (1)$$

where $G_\beta = G_F \cos\theta_C$ (with the Fermi constant G_F and the Cabibbo angle θ_C), n_i is the fraction of occupancy, C_i is the nuclear shape factor, β_i is the Coulomb amplitude of the electron radial wave function and B_i is an atomic correction for electron exchange and overlap. We have only considered the one-hole electron excitation spectrum with end-point $Q = 2.5$ keV and $m_\nu = 0$. Until very recently, the Q value was experimentally determined by the ratios of the capture probability from different atomic shells. This kind of determination is affected by large uncertainties—i.e., error on the theoretical atomic physics factors involved—so that the Q value ranged from 2.3 eV to 2.8 keV, with a recommended value of 2.555 ± 0.016 keV [7]. Only recently, the Q value has been determined from a measurement of ^{163}Ho - ^{163}Dy mass difference using the Penning trap mass spectrometer. The measured value is 2.8 keV [8].

Furthermore, the rise time of these pulses has been chosen taking into account the constraints given by both the bandwidth of the microwave multiplexing read out with a flux ramp demodulation [9] and the bandwidth of the ADC boards currently available for ROACH2 (550 MHz). Indeed, the multiplexing factor is approximately given by $0.02 f_{adc} \tau_{\text{rise}}$, where f_{adc} is the ADC bandwidth and τ_{rise} is the rise time of a TES signal. For HOLMES, a desired multiplexing factor could be 50, achievable with the performances of the ROACH2 digitizer and a τ_{rise} around 5 μs. TESs with this specification are under development at NIST.

3 Pile-Up Events

In order to study the time resolution of TES detectors, we generate sets of pile-up events with known time distances by using pulse and noise profiles described above. In first approximation, we can only consider pile up of two events (i.e., two decays in one detector too close in time so that they are mistaken as a single one with an apparent energy equal to the sum of the two decays). For ^{163}Ho the energy spectrum of pile-up events, given by the self-convolution of the calorimetric EC spectrum, is quite complex (see Fig. 3, left panel).

In fact, unresolved pile-up events cause a series of pile-up peaks close to the end-point energy. The intensity of the pile-up spectrum is given by the probability $f_{pp} = A_{EC} \tau_{\text{eff}}$, where A_{EC} is the EC activity and τ_{eff} is the effective time resolution. τ_{eff} could be estimated from the rejection efficiency $\eta(x)$, under the requirement to detect 99% of single events. The rejection efficiency is defined as the fraction of the pile-up events rejected by discrimination algorithms. Therefore, τ_{eff} is

$$\tau_{\text{eff}} = T \left[1 - \int_0^T \frac{\eta(x)}{T} dx \right] \tag{2}$$

where T is the time interval considered. In our simulations, the delay of the second event on the first one ranges from 0 to 8 μs with a step of 0.1 μs (i.e., $T = 8$ μs). Furthermore, the arrival time does not match with the sampling. In fact, the simulated signals are originally oversampled and the arrival time is generated randomly, in order to recreate a realistic situation. Finally, we have simulated events such as $E_1 + E_2 \in$

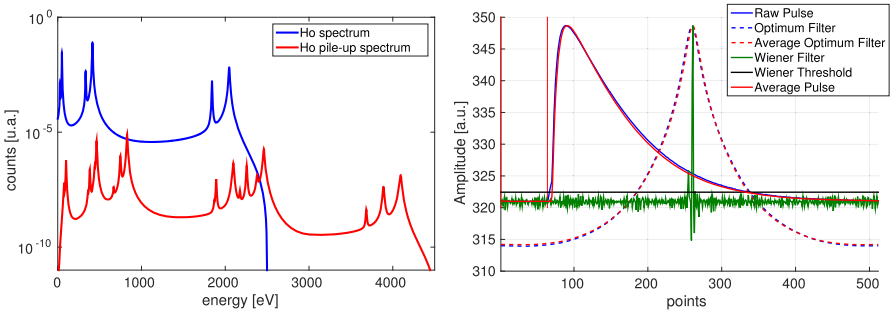

Fig. 3 *Left panel* in *blue* the ^{163}Ho decay experimental spectrum simulated for $Q = 2500$ eV, an energy resolution $\Delta E_{FWHM} = 2$ eV and $m_\nu = 0$ based on one-hole de-excitations. In *red* the ^{163}Ho pile up spectrum scaled by the relative probability $3 \cdot 10^{-4}$ of pile-up. *Right panel* a pile-up event well identified by the Wiener (*green line*) filter. In *blue dashed line* the Optimum filter output of the raw pulse while in *red dashed line* the Optimum filter output of the average pulse. In *black* the Wiener threshold for the discrimination of pile-up events (Color figure online)

$[2.4 - 2.6]$ keV. We have evaluated the pile-up discrimination close to the end-point energy, where an effect of a non-vanishing neutrino mass produces a tiny deformation of the EC spectrum.

4 ADC Simulation

In the multiplexing read out with a flux ramp demodulation, the frequency of the ramp f_r sets the effective sampling frequency of the signal f_s. To acquire pulses without distortions and without cross talk some conditions must be satisfied: the bandwidth of the resonators Δf must be at least two times f_s multiplied by the number of flux quanta per ramp, the spacing between the tones should be at least $5\Delta f$ and finally the sampling time should be at least 5 times faster than the rise time. The HOLMES read out will be capable of providing tones on a total bandwidth of 550 MHz. Under these conditions, we have simulated a 12 bit ADC with a dynamic range from 0 to 40 μA (40 μA is the expected variation of current in a TES due to a deposition of about 4 keV). We have set the sample frequencies at 1 or 2 MHz and we have chosen a record length of 1024 and 512 points, respectively. The number of points for the pre-trigger is 1/8 of the record length.

5 Pile-Up Rejection Algorithms

In our analysis the pile-up discrimination algorithms are based on the Optimum Filter and on the Wiener Filter.

– **Optimum Filter and shape parameters** The Optimum Filter (OF) [10] provides the best estimate for the signal amplitude and, as a consequence, the best energy resolution and algorithms based on it could be a good discriminator of spurious events. In the frequency domain the OF transfer function $H(\omega)$ is given by

$$H(\omega) = \eta \frac{S^*(\omega)}{N(\omega)} e^{-i\omega t_M} \tag{3}$$

where $S^*(\omega)$ is the complex conjugate of the Fourier transform of the ideal signal, $N(\omega)$ is the noise power spectrum of the main disturbs affecting the signal, t_M is the delay of the current pulse with respect to the reference pulse and η is a proper normalization constant. The OF weights the frequency components of the signal in order to suppress those frequencies that are highly influenced by noise. We evaluate $S(\omega)$ by averaging a large number of raw pulses; in this way the noise associated with each of them averages to zero. $N(\omega)$ is obtained by acquiring many baselines and averaging the corresponding power spectra. Shape parameters computed on the filtered pulse are used as tools for discarding spurious events. These parameters are the root mean square differences between the average pulse $A(t)$ and the signal $O(t)$ both after the optimum filtering. The synchronization between them is performed by making their maximum to coincide. The square differences TV of the two functions are given by Eq. (4) and they are evaluated on the right (TVR—test value right) and the left (TVL—test value left) side of the maximum on a proper time interval.

$$TV = \frac{1}{N} \sum_{i}^{N} \left(\frac{A_i - O_i}{A_{\max}} \right)^2 \tag{4}$$

where $A_{\max}$ is the maximum of the filtered average pulse.

– **Wiener Filter** The Wiener Filter (WF) technique is a digital filter to gain time resolution and its transfer function is:

$$H_i^W = \frac{S_i^*}{N_i + \alpha |S_i|^2} \tag{5}$$

where S_i and N_i are the ith discrete Fourier transform (DFT) component of the average pulse and the ith component of the noise average power spectrum, respectively. α is a parameter that depends on the energy of the signal to be filtered and it scales the average pulse power in order to be correctly compared to the noise average contribution.

We have performed simulations for different pulse shapes and for different sample frequencies. The comparison between the two rejection techniques evaluated (i.e., OF test and WF test) are reported in table 1 together with the energy resolution ΔE_{FWHM} at 2047 eV evaluated with the OF. The energy resolution has been determined simulating 10000 single mono-energetic pulses. Also in this case, the simulated signals are originally oversampled and then downsampled in order to recreate a realistic situation. In the right panel of Fig. 3 a pile-up event well identified by the Wiener Filter is displayed together with the Optimum filter outputs of the raw and average pulses.

Table 1 Comparison of different algorithms

L (nH)	τ_{rise} (μs)	f_{sample} (MHz)	rec. len. (samples)	OF test:τ_{eff} (μs)	WF test:τ_{eff} (μs)	ΔE_{FWHM} (eV)
24	2.3	2	1024	1	0.9	1.7
24*	2.3	1	512	1.8	1	3
48	4.5	1	512	4.2	1.3	2.1

OF test concerns cuts on both shape parameters (TVL, TVR). τ_{eff} has been estimated from the rejection efficiency, under the requirement to detect 99% of single events. The energy resolution ΔE_{FWHM} at 2047 eV is evaluated with the OF, simulating 10000 mono-energetic pulses affected by noise. For the simulation in the second row (*) the sampling time is only two times faster than the rise time. The scatter in energy resolution relies on the number of the samples on the rise of the pulse

6 Conclusion

Among the different rejection techniques evaluated, the Wiener Filter technique has shown an excellent pile-up rejection efficiency. For example, for a rise time of around 5 μs an effective time resolution of 1.3 μs was found. The obtained time and energy resolutions closely match the baseline specifications of the HOLMES experiment (time resolution of $\sim$ 1 μs and energy resolution of $\sim$1 eV). Other algorithms are also being tested and the results are reported in [11]. Given the good performance obtained with the WF algorithm further investigation with longer rise times are being considered in order to increase the multiplexing factor.

Acknowledgments The HOLMES experiment is funded by the European Research Council under the European Union's Seventh Framework Programme (FP7/2007-2013)/ERC Grant Agreement No. 340321. We also acknowledge support from INFN for the MARE project, from the NIST Innovations in Measurement Science program for the TES detector development.

References

1. L. Gastaldo et al., J. Low Temp. Phys. **176**, 876 (2014)
2. B. Alpert et al., Eur. Phys. J. C **75**, 112 (2015)
3. NuMECS web page. http://p25ext.lanl.gov/kunde/NuMECS/. Accessed 1 Nov 2015
4. A. Nucciotti, Eur. Phys. J. C **4**, 3161 (2014)
5. K. Irwin, G. Hilton, in *Cryogenic Particle Detection*, ed. by C. Enss (Springer, Berlin, 2005)
6. B. Shank et al., AIP Adv. **4**, 117106 (2014)
7. G. Audi, A.H. Wapstra, Nucl. Phys. A **595**, 409 (1995)
8. S. Eliseev et al., Phys. Rev. Lett. **115**, 062501 (2015)
9. O. Noroozian et al., Applied. Phys. Lett. **103**, 202602 (2013)
10. E. Gatti, P.F. Manfredi, Rivista del Nuovo Cimento **9**, 1 (1986)
11. B. Alpert et al., J. Low Temp. Phys., this Special Issue. doi:10.1007/s10909-015-1402-y